



Theory

Digital Image Content and Context Information in Tissue-based Diagnosis

Klaus Kayser¹⁾, Stephan Borkenfeld²⁾, Gian Kayser³⁾

- 1) Institute of Pathology, Charite, Berlin, Germany
- 2) International Academy of Telepathology, Heidelberg, Germany
- 3) Institute of Pathology, University of Freiburg, Freiburg, Germany

Abstract

Background and definitions: *Image content information* (ICI) comprises the information that an external observer can extract solely from the image itself, i.e., without additional notifications (labels, classification, etc.). *Image analysis* is the procedure to extract meaningful information from the image. It is an important issue in digital pathology and the prerequisite to implement algorithms of diagnosis assistance. *Meaningful information* (IMI) comprises the information which the observer can understand or which is transformed into an information related reaction. It corresponds to regions of interest (ROI). *Pixel and gray value* create all information of a digitized image. The spatial distribution of pixel gray values is called *texture*. *Objects* are externally defined pixel clusters; their spatial distribution forms a *structure*.

Living organisms are limited spatially circumscribed systems which are included in external environment and possess an unstable inner volume. Development and limited stability of these open thermodynamic systems are guaranteed by their environment and additional not overlapping inner equivalent systems, which build the so - called hierarchically order of structures. Interaction between objects might alter appearance, development, appearance of new or disappearance of existing objects. The interactions are commonly called *functions*. They are equivalent to communication and based upon different 'carriers' such as electromagnetic signals, macromolecules, salt concentrations, etc.

Detection and description of structures depend upon the observer time. The application of visible macromolecules which bind to boundaries of structures might detect and forecast changes of the boundaries, i.e. structures. The intensity of the visibility and its distribution reflect to the thermodynamic affinity. Detailed analysis of gray value intensities might allow an insight in thermodynamic properties of structures.

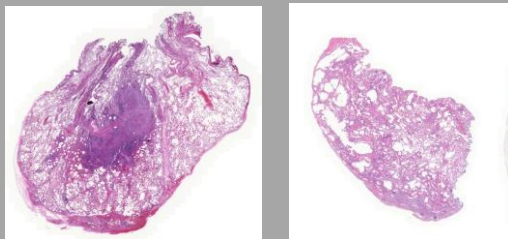
Context is defined as information which can be derived from and added to object and structure related information, and, vice versa, might be applied to predefine the observer information capability which is needed to understand the 'meaning' of an image, or to select the most capable observer.



Perspectives: The described algorithm is an appropriate tool to combine computerized image content information with its computerized 'observer' system. It will be able to measure, acquire, understand and to transfer image content information in an adequate reaction, i.e. diagnosis.

Keywords: [Tissue-based Diagnosis](#), [Image Content Information](#), [Image Context Information](#), [Image Analysis](#), [Observer Time](#).

Virtual Slides:



Introduction

The development of digital cameras and microscopic slide scanners has opened a new world of image analysis and tissue – based diagnosis. It uses the evaluation of digitized slides [1]. In addition to these 'electronic' tools advanced techniques of molecular biology and molecular genetics have induced the collection of numerous inter- and intracellular information, which require detailed statistical analysis in order to map the detected pathways in our visual understanding and practical application [2, 3].

All these approaches take advantage of the 'electronic world', i.e., the transformation of 'real nature systems' into virtual reality.

Some of these transformations rely on extensive sampling of concrete findings and behaviour of 'intelligent life', for example input data of 'deep learning' which have been developed by observation and simulation of human information acquisition (construction and function of the human brain) [4, 5].

Application of geometric transformations indicate that transformation of real life into virtual environment might be compared to transform our four dimensional space of reality (3 reversible and 1 non reversible coordinates) into a three dimensional space, which consists of 3 reversible coordinates only (2 space associated and 1 reversible time associated coordinate) [6, 7]. Thus, conventional diagnostic microscopy which works with 3-dimensional images, is mapped on two dimensional virtual microscopy. It might include several repeatable image planes (z planes). These potentially correspond to 'different 'times' and are illustrated in overlay technique [8-10].

In nature, man is forced to detect, classify and to take advantage of recognized objects and their behaviour. Otherwise he will not survive. Thus, recognition in nature requires both visualization and understanding of distinct objects and their behaviour, in other words of structures and functions. Natural sciences have to analyse structure and function in a living system, if they want to reproducibly understand and forecast the state of the system [11-15].



Both structure and function are mandatory to guarantee the present existence of creatures including man. A living system without any structure never has been detected in reality. A system without a function is called a corpse and will disappear if not appropriately conserved.

Therefore, it seems to be of advantage to define and clearly distinguish between structure and function in virtual microscopy.

Structure and function

Consider the acquisition of a complete image space (background) or of n objects $\{O_{i1}\}$ at time t_1 and position $\{x_i, y_i, z_i\}$. An object is a distinct circumscribed space which can be separated from its non - overlapping environment.

We can write: $O_{i1} = f(x_i, y_i, z_i, t_1)$.

At time t_2 ($t_2 > t_1$) the objects $\{O_{i2}\}$ can be described by the position $\{x_i, y_i, z_i\}$ $O_{i2} = f(x_i, y_i, z_i, t_2)$.

If $\sum \{O_{i2} - O_{i1}\} = 0 \rightarrow$ Structure; if $\sum \{O_{i2} - O_{i1}\} \neq 0 \rightarrow$ Function (1).

The mappings of objects at times $\{t_2, t_1\}$ form the structure, the differentials create the function.

A function is physically the equivalent to 'interactions' between structures and / or the environment. They might be induced by forces of the environment or of included objects, or of both.

Derivatives: Structures induce, preserve, alter, or delete functions.
Functions create, preserve, alter, or erase structures.
Structures require functions to be created, altered or erased.
Functions require structures to be recognized.
Structure and function are of the same entity in nature.
Their recognition depends upon the observer time.
In nature the interaction between structures is directed and not reversible.
The commutative law is not valid in series of functions.

The transformation of the situation into the virtual world will replace $f(x, y, z, t)$ by $f(x, y, r)$ and the sequence of $t_2 > t_1$ by $r = \{t_1, t_2\}$. t_1 can always be replaced by t_2 and vice versa. A function might always to be turned into a structure, because time is reversible.

In practice, the recognition of structures and functions depends upon the display of the background (magnification), which creates distinct 'hierarchy levels' and orders of structures [16-19].

The general principle of 'structural hierarchies' in nature is implemented by spatial embedding (like a Russian doll). For example, a nucleus is surrounded by cytoplasm, a cell by its membrane. Blood is transported within a vessel; nerves are surrounded by a sheath.

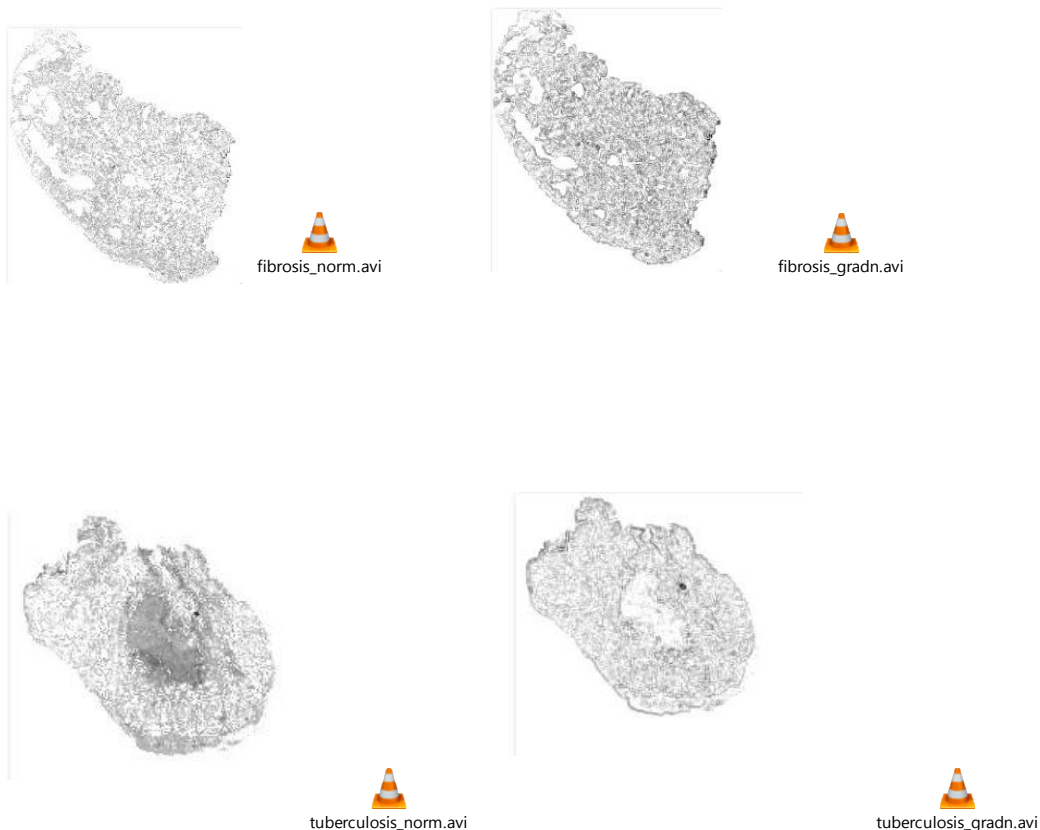
Functions are messages that are released by a 'biological significant object'. They induce changes on different objects or in the environment. The interactions between structures (functions) might occur in the same or between different 'hierarchy levels' and might display with different complexity and power [3, 14, 20-22]. The knowledge of the involved structures might forecast the fate of the whole system [23-25].



To explain in detail: Let n different structures $\{s_i\}$ been mapped in the same level. $\{s_i\}$ are distinct non overlapping elements of a finite set connected by $k(s_i s_j)$ neighbourhood relations with an individual or multiple action forces (binding power, field force, etc.) $p=f(k(s_i s_j))$ at time t . The new set of the next higher order possesses $\Sigma[(n-1) * (k(s_i s_j))]$ structures at maximum.

The structures at each level can be considered an alphabet of distinct elements, which interact and induce from bottom to top and / or upside down new created structures and functions. They form a dynamic network, which formally can be investigated to fulfil predefined conditions such as to minimize the total neighbourhood distances (length of the included trees in graph theory mapping). They might create new structures, if a neighbour is missing, or build specific sole bars which guarantee the systems equilibrium.

An exemplary example is shown in the 'motion transformed 'avi' files < avi1 – avi4>. The files avi1 and avi2 present with the gray value dependent 'structure' related pixels and are representative for the shown image information content (avi1 shows a node of an active lung tuberculosis, and avi2 an interstitial lung fibrosis). The derived functions are given in avi3 and avi4 correspondingly. There is no functional activity in the center of the tuberculosis nodule, and a diffuse activity in the lung fibrosis.



Formally, the approach reminds of a neural network including specific derivatives such a deep learning [26-29]. The more 'functions' are connected to a structure the higher is its influence on the whole system. In other words, the number and 'strength' of functions indicate the 'biological significance' of a structure.



Mapping of structures into a digital image space within a small, negligible period (snap shot) results in morphology. It is an appropriate tool to analyse different structure 'hierarchies' of the whole biological system.

How to statistically analyse the complexity of structures and to forecast the system's development?

Complexity of structures

The more complex a system the higher is its 'order' and the more complex is the amount and released information. Self - organisation such as DNA configuration might be described as loss of structures at the lower level and contemporary birth of new structures at next higher levels. The sequence {amino acids – DNA configuration – gene – chromosome – nucleus – cell – gland – stomach – body} is exemplary for biological structures.

The amount of newly created information or the number potential new structures is limited and can be calculated according to statistical laws. For example, the number of potentially created genes is defined by the number of different nuclear acids and the maximum length of the chain (number of allowed nuclear acids).

From the viewpoint of statistics, the number of structures within a certain hierarchy level corresponds to the number of microstates, that of the created 'agglutinations' (structures at the next higher hierarchy level) to that of macrostates [30-33].

Obviously, the frequency distribution of the microstates influences the frequency distribution of the macrostates. Boltzmann has described the general mathematical procedure to computing the expected and observed distributions, and to derive the corresponding coherency [32, 33].

Systems that include regulatory issues such as feedback mechanisms might release functions that start from structures at a higher order (macrostates) and involve structures at a lower order (microstates) [32, 33]. They result in changes of the frequency distribution of microstates and contemporary modulate that of the macrostates [18, 32, 34, 35].

An expansion of this simple model might include several hierarchy layers. For example, it might start at the level of atoms, followed by the series of small molecules, macromolecules, membranes and gene compartments, virus, bacteria, vessels, nerves, etc. [18, 36].

Without going into statistical details, we can expect the following effects after translation in a digital image:

1. Each hierarchy layer increases remarkably the complexity (and potentially active) functions of the system. The entropy approach indicates that it will become 'more intelligent' because it loses the freedom to react by random [33].
2. Structures located in a 'far distant' level might also involve structures in a basic layer, and vice versa.
3. Changes in 'low layer' structures' become easier 'non reversible' than structures located in higher layers, because 'they are under control'.
4. Different structures located in the same layer might interact in between without any direct interaction via structures of a different layer.



5. Focal destruction of basic layer structures might induce the collapse of the whole system (death).

The complexity of structures and associated functions is closely related to the information content of the system. It also demonstrates its 'intelligence' if it is able to react or to release consecutive signals into its environment.

How to evaluate the system's 'intelligence' and to derive meaningful information from image content information (ICI)?

Basic considerations on the entropy approach

Natural sciences aim to describe, explain and forecast the future development of an observable system, starting from its present measurable stage. Specific system properties that are successfully mapped on practical transformations commonly include quantifiable attributes (equivalent to structures) and algorithms (equivalent to functions).

Life might be considered as a thermodynamic system whose main attributes include pressure, temperature, volume and (free) energy. Appropriate algorithms would address the development of the system, forecast its final stage, and compare the obtained result with the forecast of the performed measurements [14, 32, 33, 37-41].

The entropy approach is one of these algorithms. It is a basic measure of internal statistical characteristics of a broad variety of systems. These comprise different physical realizations including linguistics, reversible and non-reversible thermodynamics, acoustics, optics, quantum physics, information technology, computation (numbers, vectors, etc.), mathematics (geometry, image analysis), sociology (income, age, etc. of defined populations), or biology (self - organization of macromolecules, or hierarchical structures, as discussed above) [39, 42-44].

In principle, the term entropy is a state variable and corresponds to the transported heat divided by the absolute temperature [45]. Its mathematical formulation varies and depends upon the presumption which properties the system's elements should possess.

The generic formula is the fluxion of transported heat divided by the absolute temperature $dS = d(Q)/T + d(W_{diss})/T$ with $D(Q)$ = additive heat and $d(W_{diss})$ = inside created heat.

The structural entropy $S(MST) = -k \cdot \sum \{p(s, \delta) \cdot \ln p(s, \delta)\}$ (2)

with $p(s, \delta)$ = probability of structure features (object size, distance, etc.).

Shannon's entropy formula is generated from ideal elements which do not occupy any space and are completely independent from each other. These theoretical conditions are called strong chaos [46-49].

Tsallis and other authors investigated in systems whose elements form a set of space occupying 'subgroups' (for example dies and numbers (so – called q-entropy)) [46-49].

Herein, the calculated entropies of the 'sub-systems' cannot simply be added, and realistic calculations might become difficult [50-52].

The entropy concept is a reliable predictor of the final stage of closed systems. The entropy flow is an equivalent appropriate predictor of open systems. Open systems are circumscribed



(limited) systems which exchange elements or properties with their environment. Any of such a system will reach its final stage if its entropy flow becomes a minimum [53].

The structural entropy and its entropy flow $SF = dS \cdot C^{-1} / dt$ (C = surface, t = time) are a useful measure to predict the outcome of operated lung cancer patients or the potential occurrence of metastases in solid tumors [33].

Measures of image content information

Image content information (ICI) is a term which solely addresses the distribution of gray values and its spatial clusters [2, 31, 44, 54]. It might be measured in each of its 3 color dimensions (for example red, green, blue, (rgb)) or in a one dimensional gray value image only [2, 31, 44, 54].

The ICI idea is that any image interpretation or diagnosis evaluation (DE) might be separated in two independent procedures: $DE = ICI \cdot EK$.

EK stays for the external knowledge of the pathologist. DE becomes zero, if $ICI=0$, and /or $DE=0$. In other words, a diagnosis can only be evaluated from the visual information of an image by a pathologist who possesses the mandatory knowledge.

The measurable image parameters include its (Shannon) entropy S , its structural entropy $S(MST)$, its entropy flows, and its spatial gray value distribution G . All parameters might be measured from both, the original and the differentiated image). The original and additional images derived from spatial dependent and / or independent transformation might serve for additional measurements of the same parameters. The obtained measurement results might be used to construct images of randomly distributed similar features and serve for additional reference data [55-57].

Exemplary examples of corresponding image measurements applied to the virtual slides are depicted in <Figures 1 - 2>.

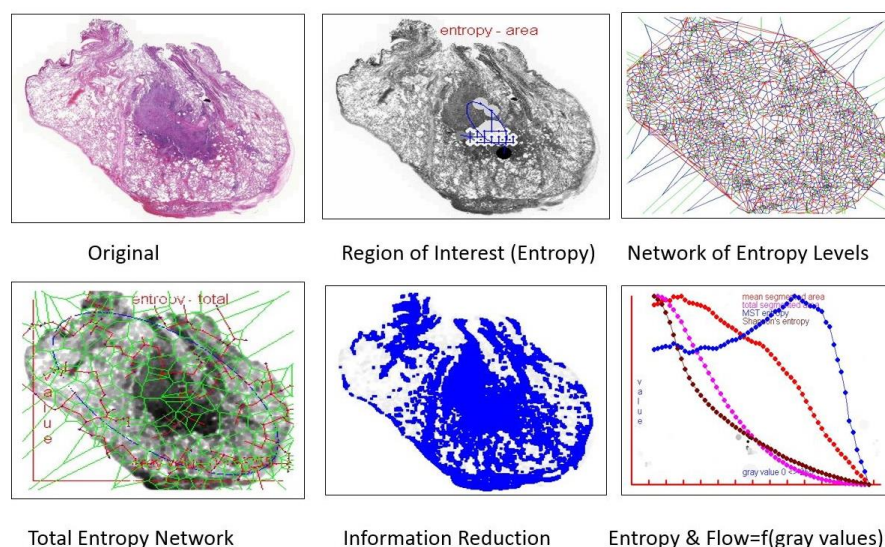


Figure 1: Tuberculosis – Context Information

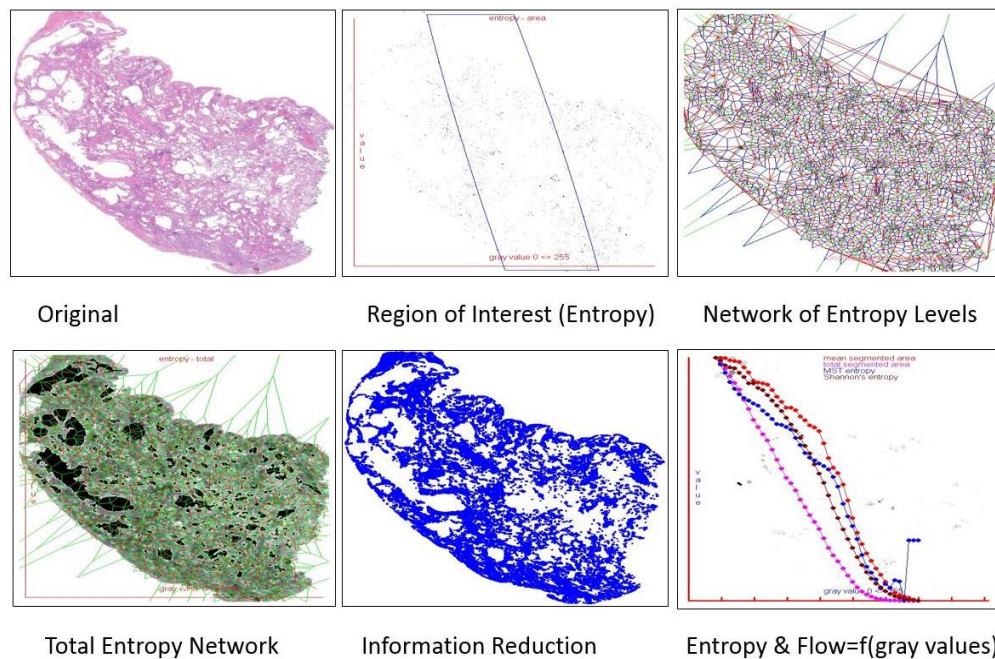


Figure 2: Interstitial Fibrosis – Context Information

Meaningful image information (IMI)

Image content information measures the absolute image information in 'itself'. It is a signal that any observer might acquire and 'translate' in his understanding or reaction, for example in a diagnosis. Obviously, the observer has to possess adequate knowledge if he wants to make reasonable use of ICI.

The intended distinction between ICI, IMI, External Context Information (ECI), and the contributions to the final derived diagnosis (DDI) might be formally written:

$$DDI = ICI * IMI * ECI; \text{ with } IMI > ICI, \text{ and } ICI > IMI \quad (3)$$

The three data sets are not completely independent from each other, because they create a hierarchic order of information. The equation (3) addresses a predefined goal which is the diagnosis and / or an active treatment of the patient.

ECI defines the goal of the information transfer, and might differ from a diagnosis, for example to perform quality evaluations, or to implement an additional level of ECI.

The principle algorithm is demonstrated in <Figure 3>.

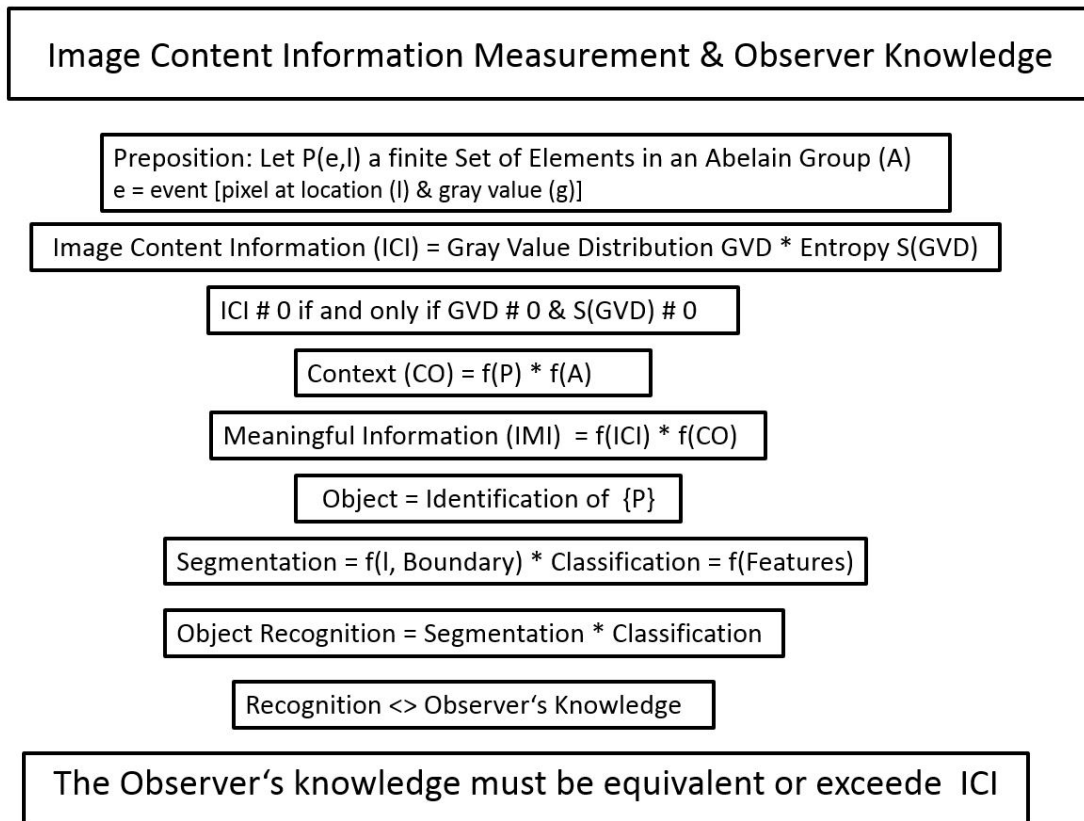


Figure 3: principle algorithm

The important task is how to connect the three information sets.

In practice, ICI provides the input data of a discriminant analysis, which is usually predefined and often specifically addresses the goal of the investigation. Examples are immune histochemical investigations (IHC) which are applied to confirm or exclude a certain diagnosis or to estimate the patients' survival [58-60].

Pathologists commonly prepare the needed investigations (for example IHC stains, in situ hybridization, etc.), select the mandatory data sets (for example cancer cell type, clinical history, treatment, etc.), choose a statistical tool which discriminates between the different data sets and calculates potential associations between the ICI data and the intended goal. Some of these tools require huge data sets, for example deep learning systems. Others might work with less numerous input data, such as algorithms which possess feedback sequences [61, 62].

All of them include IMI and ECI in their algorithm. Usually, they do not distinguish between IMI and EMI.

What is the advantage to separate IMI from ECI and to calculate IMI and ECI separately?



Image Information Context

At the first glance, microscopic ICI content seems to be a meaningless measure without a predefined goal. It is spatially either randomly, focally, or multifocal distributed.

So – called regions of interest (ROI) indicate the areas with the highest information content. In microscopy, it corresponds to the image area(s) which the pathologist is mainly interested in, i.e., which include the most useful image compartments to derive a diagnosis.

These image areas can be calculated without knowing the pathologist's experience or method of diagnosis evaluation [59, 60, 63, 64]. The algorithms which select the ROIs solely depend on image features such as pixel – associated entropy, and entropy flow, segmented image primitives, image comparison tools (including deep learning) [2, 6, 65].

Thus, the algorithms result in 'meaning - related data' without knowing the meaning itself, they correspond to a 'feature of the image itself'.

In a next step, the automatically detected ROIs might be classified by position, number, area, and in relation to the whole ICI.

In addition, these data might fed into a pushdown automation (PDA) in order to select the appropriate algorithm of the required external context information (ECI). It might also calculate the mandatory pathologist's knowledge (amount of internal information) if he wants to understand the submitted ICI, or to finally diagnose the underlying disease [66].

The measurement of ICI and ROI include a series of investigations in routine diagnostics:

1. The image quality has to be assessed by measures of gray value distribution of the whole image and its potential correction [2, 6, 65]. These might include vignette (shading) and range of gray values.
2. The applied stains have to be confirmed by the analysis of the color distribution of the whole image. Fluorescence presents with distinct color channels, IHC with enhanced color intensities dependent upon the used visualization dye [3, 31, 54, 56].
3. Different organs present with the highest order of structures. An organ might be recognized at low magnification and by measures of areas which lay out of the ROIs. Several algorithms are applicable because the set of human organs is limited and includes a total of 23 different items only.

Examples: <Figure 1> displays with a solid tumor, which is surrounded by inflammatory altered lung tissue. The measured information of the complete image and that of the detected ROIs (ICI) are also shown <Figure 1>. The PDA application results in a table which includes several circumscribed lung diseases such as tuberculosis, solid lung cancer, pseudo lymph node, infarction, fungus, etc.). The complete set of lung disease is limited and amounts to approximately 870 different diseases. The algorithm results in a reduced set of less than 50 diseases. The procedure can be repeated using a new set of image features, which are obtained by measures at a different level (magnification) and include a new 'vocabulary' of lung diseases, which includes detailed features of circumscribed lesions.

A second example is shown in <Figure 2>. Herein, a virtual slide of lung fibrosis is shown. The detected ROIs display with nearly identical ICI of the whole image. Therefore, the lesions are multifocal or randomly distributed, and the disease must be continuous and not of focal nature.



It is of advantage in routine application, to separate the different information compartments and to implement a cloud system, which analyzes the different information features separately. Several of the potentially useful algorithms are free accessible and might be implemented without greater difficulties.

Additional examples are demonstrated in <Figures 4, 5>. They exemplarily show the gray value dependent image information content and the associated Shannon entropies. Images with randomly distributed objects posses higher entropy values and a broader gray value distribution of image content information (ICI), if compared to a tuberculosis nodule or interstitial fibrosis.

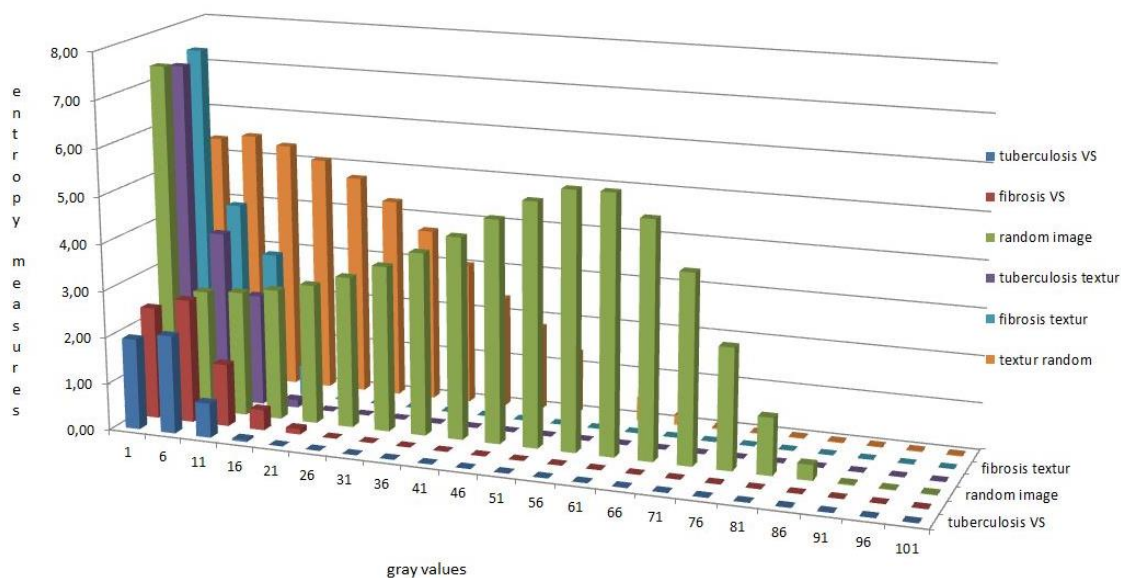


Figure 4: gray value dependent entropies in virtual slides of tuberculosis & lung fibrosis

Please note: only low gray values < 26 contribute to the entropy measures in the virtual slides of tuberculosis and fibrosis in contrast to the randomly created image.

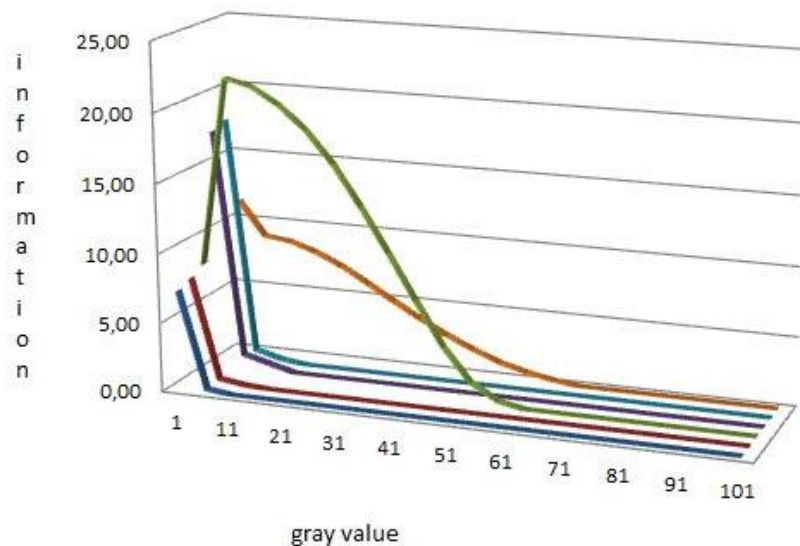


Figure 5: gray value dependent image information. Explanation:

- y-axis: gray value dependent information of the tuberculosis virtual slide
- gray value dependent information of the fibrosis virtual slide
- gray value dependent information of the random virtual slide
- texture dependent information of the tuberculosis virtual slide
- texture dependent information of the fibrosis virtual slide
- texture dependent information of the random virtual slide

x-axis: information = entropy measure * gray value volume fraction

Discussion and perspectives

The date of birth of image analysis algorithms is probably the development and implementation of stereology in 1960 and afterwards [1, 67-69]. The intention was to derive three dimensional properties such as volume fraction from two dimensional fractions [68]. However, stereology has never been used in routine surgical pathology diagnosis to a larger extent.

The development of digital cameras and whole slide scanners as well as the implementation of electronic communication standards (internet, DICOM, etc.) promoted the intention to take advantage of data mapping into a virtual environment. Virtual slide scanners are implemented in nearly all greater pathology institutes of the Western Countries. No major international pathology conference exists without extensive discussion of digital pathology [70].

Most pathologists are familiar with virtual microscopy and electronic image transfer within a hospital. They also accept that the recently implemented molecular genetic tools remarkably contribute to refinement of tissue – based diagnosis. Some of these developed techniques such as liquid biopsies or in vivo biopsies are already entering the clinical practice.



On the other hand, most pathologists are still convinced that at least the ‘over all control’ of electronically derived diagnosis will remain in their hands ‘forever’. Their opinion seems to be supported by the recently implemented ‘deep learning systems’, which commonly address specific diagnostic tasks only, and might still be considered ‘diagnosis assistants’ [70].

However, a look into the history of deep learning already awakes doubts that this will be the end of the virtual development [2, 6, 55, 71].

Theoretical considerations on ‘neural networks’ have been published already 30 years ago or even earlier. Already in 1994 C. Krylow edited presentations of a conference on ‘advances in synergetics’ and discussed nonlinear collective dynamics in neural networks [26, 57]. Adding widely known algorithms such as the Cocke-Younger-Kasami method to the free accessible ‘deep learning systems’, the ideas of Turing machines and PDA algorithms opened the gate to understand, why and how the virtual world will give birth to self - development of its implemented tasks. In other words, self – development which corresponds to self - reproduction is not limited to biology systems. To the contrary, it seems to be a natural entity which can be mapped to virtual environments too.

Finally, the detection of context and its transformation into knowledge is no human privilege. It is a property of nature and will probably develop its own dynamics. The new virtual world of digital tissue – based diagnosis will stay at the level of a useful and helpful assistant as long as it will not create its own ‘goals’, or present with its own ‘ethics’. An important task of digital tissue – based diagnosis in the near future is to ascertain that ‘computer ethics’ will remain identical to ‘human ethics’.

References

1. [Kayser, K., et al., History and structures of telecommunication in pathology, focusing on open access platforms. Diagn Pathol. 6: p. 110.](#)
2. [Kayser, K., Quantification of virtual slides: Approaches to analysis of content-based image information. J Pathol Inform. 2: p. 2.](#)
3. [Kayser, K., et al., Grid computing in image analysis. Diagn Pathol. 6 Suppl 1: p. S12.](#)
4. [Achille, A. and S. Soatto, Information Dropout: Learning Optimal Representations Through Noisy Computation. IEEE Trans Pattern Anal Mach Intell, 2018.](#)
5. [Aggarwal, H.K., M.P. Mani, and M. Jacob, MoDL: Model Based Deep Learning Architecture for Inverse Problems. IEEE Trans Med Imaging, 2018.](#)
6. [Kayser, K., et al., Texture and object related image analysis in microscopic images. Diagnostic Pathology, 2015. 1\(14\).](#)
7. [Kayser, K., et al., To be at the right place at the right time. Diagn Pathol. 6: p. 2-9.](#)
8. [Al-Kofahi, Y., et al., A deep learning-based algorithm for 2-D cell segmentation in microscopy images. BMC Bioinformatics, 2018. 19\(1\): p. 365.](#)
9. [Bellenberg, S., et al., Automated Microscopic Analysis of Metal Sulfide Colonization by Acidophilic Microorganisms. Appl Environ Microbiol, 2018. 84\(20\).](#)



10. [Nelson, A.J. and S.T. Hess, *Molecular imaging with neural training of identification algorithm \(neural network localization identification\)*. Microsc Res Tech, 2018.](#)
11. [Kayser, G., et al., *Towards an automated morphological classification of histological images of common lung carcinomas*. Elec J Pathol Histol, 2002. **8**: p. 022-03.](#)
12. [Kayser, K., et al., *Correlation of expression of binding sites for synthetic blood group A-, B- and H-trisaccharides and for sarcolectin with survival of patients with bronchial carcinoma*. Eur J Cancer, 1994. **30A**\(5\): p. 653-7.](#)
13. [Kayser, K., et al., *Cell type-dependent alterations of binding of synthetic blood group antigen-related oligosaccharides in lung cancer*. Glycoconj J, 1994. **11**\(4\): p. 339-44.](#)
14. [Kayser, K. and H.J. Gabius, *The application of thermodynamic principles to histochemical and morphometric tissue research: principles and practical outline with focus on the glycosciences*. Cell Tissue Res, 1999. **296**\(3\): p. 443-55.](#)
15. [Kayser, K., et al., *Alterations in human lung parenchyma after cytostatic therapy*. Apmis, 1991. **99**\(2\): p. 121-8.](#)
16. [Kayser, K., S. Borkenfeld, and G. Kayser, *How to introduce virtual microscopy \(VM\) in routine diagnostic pathology: constraints, ideas, and solutions*. Anal Cell Pathol \(Amst\). **35**\(1\): p. 3-10.](#)
17. [Kayser, K., et al., *Interactive and automated application of virtual microscopy*. Diagn Pathol. **6 Suppl 1**: p. S10.](#)
18. [Kayser, K. and H. Hoffgen, *Pattern recognition in histopathology by orders of textures*. Med Inform \(Lond\), 1984. **9**\(1\): p. 55-9.](#)
19. [Kayser, K., et al., *Phenotype and genotype associations of lung carcinoma with atypical adenomatoid hyperplasia, squamous cell dysplasia, and chromosome alterations in non-neoplastic bronchial mucosa*. Rom J Morphol Embryol, 2005. **46**\(1\): p. 5-10.](#)
20. [Gabius, H.J., et al., *Reverse lectin histochemistry: design and application of glycoligands for detection of cell and tissue lectins*. Histol Histopathol, 1993. **8**\(2\): p. 369-83.](#)
21. [Kayser, K., et al., *Preneoplasia-associated expression of calcyclin and of binding sites for synthetic blood group A/H trisaccharide--exposing neoglycoconjugates in human lung*. Cancer Biochem Biophys, 1997. **15**\(4\): p. 235-43.](#)
22. [Kayser, K., et al., *Analysis of soft tissue tumors by an attributed minimum spanning tree*. Anal Quant Cytol Histol, 1991. **13**\(5\): p. 329-34.](#)
23. [Kayser, K., et al., *Alteration of human lung parenchyma associated with primary biliary cirrhosis*. Zentralbl Pathol, 1993. **139**\(4-5\): p. 377-80.](#)
24. [Kayser, K., et al., *Application of computer-assisted morphometry to the analysis of prenatal development of human lung*. Anat Histol Embryol, 1997. **26**\(2\): p. 135-9.](#)
25. [Kayser, K., et al., *Biotinylated epidermal growth factor: a useful tool for the histochemical analysis of specific binding sites*. Histochem J, 1990. **22**\(8\): p. 426-32.](#)



26. Krylow, G. *Advances in Synergetics*. in *First Workshop on Mind, Brain and Neurocomputers*. 1994. Minks, Belarus: Belarusian State University Press.
27. [Cheng, H.C., et al., *Deep-learning-assisted Volume Visualization*. IEEE Trans Vis Comput Graph, 2018.](#)
28. [Funke, J., et al., *Large Scale Image Segmentation with Structured Loss based Deep Learning for Connectome Reconstruction*. IEEE Trans Pattern Anal Mach Intell, 2018.](#)
29. [Fuyong, X., et al., *Deep Learning in Microscopy Image Analysis: A Survey*. IEEE Trans Neural Netw Learn Syst, 2018. **29**\(10\): p. 4550-4568.](#)
30. [Kayser, G., et al., *Numerical and structural centrosome aberrations are an early and stable event in the adenoma-carcinoma sequence of colorectal carcinomas*. Virchows Arch, 2005. **447**\(1\): p. 61-5.](#)
31. [Kayser, K., et al., *How to measure image quality in tissue-based diagnosis \(diagnostic surgical pathology\)*. Diagn Pathol, 2008. **3** Suppl 1: p. S11.](#)
32. [Kayser, K., et al., *Texture- and object-related automated information analysis in histological still images of various organs*. Anal Quant Cytol Histol, 2008. **30**\(6\): p. 323-35.](#)
33. [Kayser, K., G. Kayser, and K. Metze, *The concept of structural entropy in tissue-based diagnosis*. Anal Quant Cytol Histol, 2007. **29**\(5\): p. 296-308.](#)
34. [Kayser, K., et al., *Expression of endogenous lectins \(galectins, receptors for ABH-epitopes\) and the MIB-1 antigen in esophageal carcinomas and their syntactic structure analysis in relation to post-surgical tumor stage and lymph node involvement*. Anticancer Res, 2001. **21**\(2B\): p. 1439-44.](#)
35. [Kayser, K., et al., *Combined analysis of tumor growth pattern and expression of endogenous lectins as a prognostic tool in primary testicular cancer and its lung metastases*. Histol Histopathol, 2003. **18**\(3\): p. 771-9.](#)
36. [Kayser, K. and O. Hagemeyer, *Stage related morphometry of sarcoid granulomas and inflammatory cell types in broncho-alveolar lavage*. Anal Cell Pathol, 1991. **3**\(6\): p. 335-42.](#)
37. [Pincus, S.M., *Approximate entropy as a measure of system complexity*. Proc Natl Acad Sci U S A, 1991. **88**\(6\): p. 2297-2301.](#)
38. [Shannon, C., *A mathematical theory of communication*. The Bell System Technical Journal 1948. **27**\(3\): p. 379-423.](#)
39. [Eigen, M., *Selforganization of matter and the evolution of biological macromolecules*. Naturwissenschaften, 1971. **58**: p. 465-523.](#)
40. [Gibbs, J., *Elementary Principles in statistical Mechanics developed with especial reference to the rational. Foundation of Thermodynamics* 1902, New York: Yale University Press.](#)
41. [Tsallis, C., *Entropic nonextensivity: a possible measure of complexity*. Chaos, Solitons and Fractals 2002. **13**\(371-391\).](#)
42. [Beretta, G.P., *Steepest entropy ascent model for far-nonequilibrium thermodynamics: unified implementation of the maximum entropy production principle*. Phys Rev E Stat Nonlin Soft Matter Phys. **90**\(4\): p. 042113.](#)



43. [Gündüz, G. and U. Gündüz, *The mathematical analysis of the structure of some songs* Physica A, 2005. **357**: p. 565-592.](#)
44. [Kayser, K. and H.J. Gabius, *Graph theory and the entropy concept in histochemistry. Theoretical considerations, application in histopathology and the combination with receptor-specific approaches.* Prog Histochem Cytochem, 1997. **32**\(2\): p. 1-106.](#)
45. [Rocha, L.B., et al., *Shannon's entropy and fractal dimension provide an objective account of bone tissue organization during calvarial bone regeneration.* Microsc Res Tech, 2008. **71**\(8\): p. 619-25.](#)
46. [Bento, E.P., et al., *Third law of thermodynamics as a key test of generalized entropies.* Phys Rev E Stat Nonlin Soft Matter Phys, 2015. **91**\(2\): p. 022105.](#)
47. [Lima, J.A., R. Silva, and A.R. Plastino, *Nonextensive thermostatics and the H theorem.* Phys Rev Lett, 2001. **86**\(14\): p. 2938-41.](#)
48. [Mayoral, E. and A. Robledo, *Tsallis' q index and Mori's q phase transitions at the edge of chaos.* Phys Rev E Stat Nonlin Soft Matter Phys, 2005. **72**\(2 Pt 2\): p. 026209.](#)
49. [Tsekouras, G.A. and C. Tsallis, *Generalized entropy arising from a distribution of q indices.* Phys Rev E Stat Nonlin Soft Matter Phys, 2005. **71**\(4 Pt 2\): p. 046144.](#)
50. [Chavanis, P.H., *Generalized thermodynamics and Fokker-Planck equations: applications to stellar dynamics and two-dimensional turbulence.* Phys Rev E Stat Nonlin Soft Matter Phys, 2003. **68**\(3 Pt 2\): p. 036108.](#)
51. [Crupi, V., et al., *Generalized Information Theory Meets Human Cognition: Introducing a Unified Framework to Model Uncertainty and Information Search.* Cogn Sci, 2018.](#)
52. [Hasegawa, H.H., T. Nakamura, and D.J. Driebe, *Generalized second law for a simple chaotic system.* Chaos, 2017. **27**\(10\): p. 104606.](#)
53. De Groot, S.R., *Thermodynamik irreversibler Prozesse.* 1960, Mannheim: Bibliographisches Institut.
54. [Kayser, K., et al., *AI \(artificial intelligence\) in histopathology--from image analysis to automated diagnosis.* Folia Histochem Cytobiol, 2009. **47**\(3\): p. 355-61.](#)
55. [Ahar, A., A. Barri, and P. Schelkens, *From Sparse Coding Significance to Perceptual Quality: A New Approach for Image Quality Assessment.* IEEE Trans Image Process, 2018. **27**\(2\): p. 879-893.](#)
56. [Bhateja, V., et al., *Multispectral medical image fusion scheme based on hybrid contourlet and shearlet transform domains.* Rev Sci Instrum, 2018. **89**\(8\): p. 084301.](#)
57. [Mehre, S.A., et al., *Content-Based Image Retrieval System for Pulmonary Nodules Using Optimal Feature Sets and Class Membership-Based Retrieval.* J Digit Imaging, 2018.](#)
58. [Kumar, R.K., et al., *Virtual microscopy for learning and assessment in pathology.* J Pathol, 2004. **204**\(5\): p. 613-8.](#)
59. [Nakane, K., et al., *Homology-based method for detecting regions of interest in colonic digital images.* Diagn Pathol, 2015. **10**: p. 36.](#)



60. [Theart, R.P., et al., *Improved region of interest selection and colocalization analysis in three-dimensional fluorescence microscopy samples using virtual reality*. PLoS One, 2018. **13**\(8\): p. e0201965.](#)
61. [Kayser, K., et al., *Neighborhood analysis of low magnification structures \(glands\) in healthy, adenomatous, and carcinomatous colon mucosa*. Pathol Res Pract, 1986. **181**\(2\): p. 153-8.](#)
62. [Kayser, K., et al., *Combined morphometrical and syntactic structure analysis as tools for histomorphological insight into human lung carcinoma growth*. Anal Cell Pathol, 1990. **2**\(3\): p. 167-78.](#)
63. [Corredor, G., E. Romero, and M. Iregui, *An adaptable navigation strategy for Virtual Microscopy from mobile platforms*. J Biomed Inform.](#)
64. [Wright, A.I., H.I. Grabsch, and D.E. Treanor, *RandomSpot: A web-based tool for systematic random sampling of virtual slides*. J Pathol Inform. **6**: p. 8.](#)
65. [Kayser, K., *Introduction of virtual microscopy in routine surgical pathology--a hypothesis and personal view from Europe*. Diagn Pathol. **7**: p. 48.](#)
66. [John E. Hopcroft, J.D.U., *Einführung in die Automatentheorie, Formale Sprachen und Komplexitätstheorie* Vol. 3. Auflage. 1996, Bonn Addison-Wesley.](#)
67. [Kayser, K., et al., *Image standards in tissue-based diagnosis \(diagnostic surgical pathology\)*. Diagn Pathol, 2008. **3**: p. 17.](#)
68. [Kayser, K., et al., *From telepathology to virtual pathology institution: the new world of digital pathology*. Rom J Morphol Embryol, 1999. **45**: p. 3-9.](#)
69. [Park, S., et al., *The history of pathology informatics: A global perspective*. J Pathol Inform. **4**: p. 7.](#)
70. [Kayser, K., *travels on Conferences*. 2016, Berlin: schaefermueller publishing GmbH.](#)
71. [Gortler, J., et al., *Grid technology in tissue-based diagnosis: fundamentals and potential developments*. Diagn Pathol, 2006. **1**: p. 23.](#)